Analysis and Design of URLLC with Massive MIMO at Finite Blocklength

A Project Report

submitted by

THOTADA VAMSI PRIYANKA (EE19M030)

in partial fulfilment of the requirements

for the award of the degree of

MASTER OF TECHNOLOGY

DEPARTMENT OF ELECTRICAL ENGINEERING
INDIAN INSTITUTE OF TECHNOLOGY MADRAS

JUNE 2021

CERTIFICATE

This is to certify that the thesis (or project report) titled **Analysis and Design of URLLC with Massive MIMO at Finite Blocklength**, submitted by **Thotada Vamsi Priyanka (EE19M030)**, to the Indian Institute of Technology Madras, for the award of the degree of **Master of Technology**, is a bona fide record of the research work done by her under my supervision. The contents of this thesis (or project report), in full or in parts, have not been submitted to any other Institute or University for the award of any degree or diploma.

Place: Chennai

Date: 18th June 2021

Dr. SRIKRISHNA BHASHYAM
Project Guide
Professor
Dept. of Electrical Engineering
IIT Madras, 600 036

ACKNOWLEDGEMENTS

I am greatly indebted to Dr. Srikrishna Bhashyam for guiding me through the entire course of my M.Tech. project. He always took the time and effort to give me valuable suggestions, motivation and insights throughout the project. His valuable remarks and support always gave new directions to my project.

I am thankful to all the professors whose courses helped me improve my knowledge in Wireless Communication and Signal Processing through the course of the two years of my M.Tech program. Their classes always inspired me to think beyond classrooms into more practical scenarios.

A special thanks to Dr. Arun Pachai Kannu and Dr. Pradeep Kiran Sarvepalli for their encouragement and valuable suggestions in all reviews. A special word of thanks to my family and all the wonderful people I met at IITM without whom life would not have been the same.

ABSTRACT

KEYWORDS: Ultra reliable low latency communications, massive MIMO, finite blocklength information theory, nearest neighbor decoding, saddlepoint approximation, outage probability, pilot contamination, MR and MMSE processing, asymptotic analysis.

Massive MIMO for high throughput communications were largely depending on unlimited blocklength information theoretic constraints. This assumption makes it problematic for deploying Massive MIMO for ultra-reliable low latency communications (URLLC) which use short blocklength codes. Using the saddlepoint approximation, this thesis implements the framework for characterization of the error probability possible in both Uplink and Downlink scenarios of Massive MIMO at finite blocklength. [fbl]. Error probability and network availability using UCA in addition to that of ULA in the paper is shown. The framework in the paper consists of imperfect channel state information(I-CSI), spatially correlated channels, pilot contamination and arbitrary linear spatial processing. With minimum mean square error (MMSE) processing and spatially correlated channels and pilot contamination, error probability goes to zero as the number M of antennas grows to infinity at finite blocklength, which is consistent with previous results based on infinite blocklength bounds. When the channel covariance matrix is not known at the receiver, then LS channel estimation followed by Regularized zero forcing is done. MR processing is not sufficient for URLLC constraints.

TABLE OF CONTENTS

Table of Contents (continued) **Page**

LIST OF FIGURES

ABBREVIATIONS

MIMO	Multiple Input Multiple Output
URLLC	Ultra Reliable Low Latency Communications
MMSE	Minimum Mean Squared Error
MR	Maximum Ratio
UE	User Equipment
BS	Base Station
AWGN	Additive White Gaussian Noise
RCUs	Random Coding Union Bound with parameter s
SNN	Scaled Nearest neighbour
MGF	Moment Generating function
TDD	Time Division Duplex
SNR	Signal to Noise Ratio
SIR	Signal to interference Ratio
CSI	Channel State Information
ULA	Uniform Linear Array
UCA	Uniform Circular Array

NOTATION

$\mathcal{CN} \sim (0, \sigma^2)$	Complex Gaussian random variable with mean zero and variance σ^2
$\mathbf{E}[.]$	Expectation of operator
$\mathbf{P}[.]$	Probability of a set
log(.)	Natural logarithm
Q(.)	Gaussian Q-function
$\|\mathbf{X}\|_F$	Frobenius norm of matrix $\mathbf{X}$
$\|\mathbf{X}\|_2$	spectral norm of matrix $\mathbf{X}$
$(\mathbf{X})^T$	Transpose of matrix $\mathbf{X}$
$(\mathbf{X})^*$	complex conjugate of matrix $\mathbf{X}$
$(\mathbf{X})^H$	Hermitian transpose of matrix $\mathbf{X}$
$\stackrel{d}{=}$	Equality in distribution
$a_n \asymp b_n$	$\lim_{n\to\infty}(a_n - b_n) = 0$ almost surely (a_n & b_n are random sequences)

CHAPTER 1

INTRODUCTION

Next-generation wireless communication systems are expected to interconnect a wide range of devices under the Internet of Things (IoT) paradigm, ranging from vehicles or drones that will operate in high-mobility scenarios to autonomous machines or static sensors that will operate in low-mobility scenarios Durisi *et al.* (2016*a*). Traditional wireless communication technologies, such as fourth-generation (4G) Long-Term Evolution (LTE) or WiFi, prioritise data transmission rates over latency. As a result, a long-packet assumption is considered feasible, and capacity and outage capacity provide precise benchmarks for the throughput achievable in such systems. Furthermore, when transferring large packets, the length of metadata (additional information supplied in packets to ensure proper communication protocol operation) is insignificant in comparison to the length of information payload contained in each packet. As a result, less-than-optimal metadata encoding has no effect on efficiency. However, driven by new services and applications that demand low latency and high reliability, the fifth generation (5G) of wireless communication systems aims to deliver not only higher data rates, but also short-packet transmission, in which metadata can play an important role because its size is comparable to that of the information payload. Specifically, 5G systems will support three main services, namely, enhanced mobile broadband(eMBB), massive machine-type communications (mMTC), and ultra-reliable low-latency communications (URLLC) Popovski *et al.* (2018)

Very high data rates as well as moderate data rates for cell edge users must be provided in eMBB while retaining reasonable dependability, i.e., probability of error of roughly 10^{-3}. This service is a natural extension of 4G, in which devices are expected to be turned on for long periods of time. As previously stated, capacity and outage capacity are suitable benchmarks for these objectives. Enlarging the transmission bandwidth is the simplest approach to boost data speeds. However, since the radio frequency band is

crowded, several solutions have been considered. Examples are massive multiple input multiple output (MIMO), optical wireless communication (OWC) and the employment of more advanced coding methods and modulations.

In mMTC, a large number of low-rate devices will be engaged sporadically over very short periods of time, with error probabilities of roughly 10^{-1}. As a result, this service will necessitate the transmission of extremely small packets. The devices in URLLC will send brief packets at low rates, aiming for error probability of less than or equal to 10^{-5}. The devices could transmit intermittently with periodic control messages in URLLC, but the key distinction from mMTC is the lesser number of devices that will be linked to the network. Traditional asymptotic information theoretical assessments based on capacity and outage capacity do not give acceptable benchmarks for mMTC and URLLC, which require the transmission of small packets. As a result, a more sophisticated analysis of the maximum coding rate as a function of block length, known as finite-block length analysis, is required for low-latency wireless communications.

1.1 Massive MIMO

Multi-user MIMO has a number of advantages over point-to-point MIMO. Multi-user MIMO does not require a dense scattering environment, may be used with low-cost single-antenna terminals, and resource allocation is straightforward because active terminals utilise all of the time-frequency bins. However, with nearly equal numbers of service antennas and terminals and via FDD, multi-user MIMO is not a scalable technique. Massive MIMO (also known as large scale antenna systems, very large MIMO, hyper MIMO, full dimension MIMO, and ARGOS) deviates significantly from existing practise by employing a huge number of service antennas over active terminals and using TDD. Extra antennas assist by concentrating energy into smaller and smaller areas of space. This increases the efficiency and throughput of radiated energy. The expected throughput is determined by the propagation environment, which provides the terminals with asymptotically orthogonal channels. Larsson *et al.* (2014).

Other benefits of massive MIMO include

- Massive MIMO can be built with low-power, inexpensive components.
- Massive MIMO allows for a large reduction in air interface latency.
- Massive MIMO simplifies the multiple access layer.
- MMassive MIMO improves the robustness of the system against both unintentional and purposeful jamming.

Limiting Factors of Massive MIMO

- Channel Reciprocity
- Pilot Contamination
- Radio Propagation and Orthogonality of Channel Responses (Massive MIMO relies on a property of the radio environment termed favourable propagation to a great extent. Favorable propagation indicates that the propagation channel responses from the base station to distinct terminals are sufficiently diverse.)

Massive MIMO technology offers tremendous advantages in terms of energy efficiency, spectrum efficiency, resilience, and dependability. It allows for the employment of low-cost hardware at both the base station and the mobile unit side. At the base station, expensive and powerful but power-inefficient gear is replaced by a large array of low-cost, low-power components that work in unison. There are still hurdles remaining to reach the full potential of the technology, for example, computational complexity, realisation of distributed processing algorithms, and synchronisation of the antenna units.

1.2 State of the Art

Obtaining a closed-form statement of the maximum coding rate for the majority of channel models of interest is out of reach. As a result, there are two basic approaches to describing the maximum coding rate as a function of block length.

1.2.1 Non asymptotic bounds:

The area in which the maximum coding rate lies for a given error probability and block length can be described by determining upper and lower bounds on the maximum cod-

ing rate. These bounds are frequently described in terms of tail probabilities of sums of independent and identically distributed (i.i.d.) random variables, and they must be computed numerically using computationally costly processes. Polyanskiy *et al.* (2010), Durisi *et al.* (2016*b*) contains non asymptotic bounds for a variety of channel models. The meta-converse (MC) bound and the random coding union bound (RCU_s) with parameter s are the non asymptotic bounds discussed. For a fixed error probability and blocklength, the MC bound and the RCU_s limit give an upper and lower bound on the maximum coding rate, respectively.

1.2.2 Refined asymptotic expansions:

As the blocklength expands, perform asymptotic expansions of the error probability or maximum coding rate that get more accurate. For a fixed coding rate, such expansions are often accessible in closed form and describe how the maximum coding rate converges to capacity or how the error probability diminishes as the block length grows. The tail probabilities occurring in the non asymptotic bounds are frequently expanded to achieve the refined asymptotic expansions. One alternative is to investigate the maximum coding rate as a function of blocklength by imposing a reliability constraint on the blocklength and using the limit as the blocklength approaches infinity. The max coding rate $R^*(n,\epsilon)$ at which data may be conveyed using an error-correcting code of a fixed blocklength n, with a block-error probability not more than ϵ, can be increased as follows for various channels with positive finite capacity C.

$$R^*(n,\epsilon) = C - \sqrt{\frac{V}{n}}Q^{-1}(\epsilon) + \mathcal{O}\left(\frac{\log n}{n}\right) \tag{1}$$

where V denotes the channel dispersion which is variance of $\imath(X_j, Y_j)$ w.r.t same distribution given by $V = Var[\imath(X_j, Y_j)] = \frac{1}{\sqrt{2\pi}} \int e^{-z^2/2}(log2 - log(1+e^{-2\rho-2z\sqrt{\rho}}))^2 dz - C^2$, where the random variables $\imath(X_j, Y_j)$ are indep and identically distributed and X_j is drawn according to capacity distribution and Y_j is channel output and $\mathbf{E}[\imath(X_j, Y_j)]$ is the channel capacity denoted by $C = \frac{1}{\sqrt{2\pi}} \int e^{-z^2/2}(log2 - log(1 + e^{-2\rho-2z\sqrt{\rho}}))^2 dz$ for a bi-AWGN channel. $Q^{-1}(.)$ denotes the inverse of the Gaussian Q function, and

O((logn)/n) comprises terms that decay no slower than (logn)/n . The approximation that follows from (1) by omitting the O((logn)/n) term is regarded as normal approximation. If it isn't ignored, the resulting normal approximation is known as Refined normal approximation, and it performs better than a normal approximation. For short error-correcting codes, the normal approximation has served as a standard. This high-SNR normal approximation for non coherent single-antenna Rayleigh block-fading channels is accurate for probability of error above 10^{-3} and SNR values more than or equal to 15 dB, as demonstrated by numerical examples in Lancho *et al.* (2020*a*). Studying the exponential decay of the error probability by fixing the coding rate as the blocklength approaches infinity is a second way to acquire finer asymptotic expansions.

When the rate is close to capacity and n is large, normal estimates are often correct for moderate error probability and when the rate is close to capacity. For short block codes, i.e. when n is small, it does not provide a good estimate. In contrast, error exponents are correct at moderate coding rates and when the probability of error is near to zero. URLLC services run at error probability of roughly 0^{-5} and SNR values of around 0 dB Popovski *et al.* (2018). Both normal approximations and error exponents may become inaccurate for these values, making them poor benchmarks for short error-correcting codes. Using them as a benchmark for the maximum coding rate or the probability of error in the analysis and optimization of short-packet communication systems may result in incorrect results. As a result, with error probabilities below 10^{-5} and SNR values near to 0 dB, refined approximations that characterise the coding rate are required.

Though the majority of Massive MIMO material focuses on the ergodic regime, Karlsson *et al.* (2018), Bana *et al.* (2018) assume that the fading channel maintains constant during the transmission of a codeword (quasi-static fading scenario) and utilise outage capacity as asymptotic performance metric. Although the quasi-static fading scenario may be a reasonable assumption for URLLC, the infinite blocklength assumption may lead to inaccurate error probability calculationsYang *et al.* (2014). Over quasi-static fading channels, the difference between the outage capacity and the maximum coding rate feasible at finite blocklength approaches zero significantly faster than the

difference between the capacity and the maximum coding rate achievable over additive white Gaussian noise (AWGN) channels Yang *et al.* (2014). The reason for this is that the most common source of errors in quasi-static fading channels is deep-fade events, which cannot be eliminated by using channel codes, as channel coding only protects against AWGN. Applying this finding to Massive MIMO can be troublesome since channel hardening can make effective channel equivalent to an AWGN channel. The outage-capacity framework acquires CSI by employing pilot sequences. In quasi-static fading channels, CSI can be trained completely at the receiver in the asymptotic limit of large blocklength with no penalty on rate . The number of pilot symbols grow sublinearly with blocklength. Theoretically, incorporating channel-estimation overhead into the outage configuration according to Karlsson *et al.* (2018), Bana *et al.* (2018) may not be compelling. The framework must incorporate the use of a mismatch receiver that treats the channel estimate obtained using a set number of pilot symbols as perfect in the Finite blocklength regime. The typical result of interpreting the channel estimate error as noise to bound the mutual information in the ergodic situation does not apply to the outage scenario Lapidoth and Shamai (1999). In an outage scenario, this is due to the channel remaining constant during the codeword, but we're interested in computing an outage event over fading realisations. When computing bounds on the instantaneous spectral efficiency, the channel and its estimate must be viewed as deterministic quantities.

In the finite blocklength regime, the limitations of both outage and ergodic settings can be avoided by undertaking a nonasymptotic analysis of the probability of error based on the finite-blocklength information-theoretic restrictions presented in Polyanskiy *et al.* (2010) and have been extended to fading channels. in Yang *et al.* (2014), Durisi *et al.* (2016*b*), Östman *et al.* (2019). This approach has been done in Zeng *et al.* (2020), Ren *et al.* (2020). The analysis in these articles, however, is based on normal approximation Polyanskiy *et al.* (2010), whose tightness for the spectrum of probabilities of mistake in URLLC is debatable. Furthermore, the use of the normal approximation for the scenario of imperfect CSI in both 8854835 and Ren *et al.* (2020) is not convincing, because the estimate is based solely on the variance and not on the instantaneous channel estimation error. This scenario is not adaptive if the channel remains consistent

throughout the codeword period.

1.3 Outline

A strong upper bound on the error probability by adapting the random coding union bound with parameter s (RCUs) described in Martinez and i Fàbregas (2011) to the case of Massive MIMO communications. The consequence bound is true for any linear processing technique and any pilot-based channel estimation scheme, and it may be applied to Gaussian codebooks. Consider following encoding scheme for bi-AWGN channel: Encoder: $\{1, 2, \ldots, 2^k\} \rightarrow \{-1, 1\}^n$ which maps an information message $\in \{1, 2, \ldots, 2^k\}$ into n BPSK symbols. This set of n dimensional codewords created by the encoder is called as codebook with blocklength n. A decoder $\mathbf{R} \rightarrow \{1, 2, \ldots, 2^k\}$ maps received sequence into a message or an error if it satisfies $\mathbf{P}\{\hat{j} \neq j\} < \epsilon$ where ϵ is packet error probability. The bounds are numerically impractical to evaluate since they exist in the form of integrals that are unknown in closed form. An readily computed approximation is obtained using the saddlepoint method. wfe. With the use of poor channel state information, pilot contamination, and spatially correlated channels, the error probability in the uplink (UL) and downlink (DL) of a Massive MIMO network is then analysed using the bound. Both maximum ratio (MR) and minimum mean-square error (MMSE) processing are taken into account. If the transmitter does not have channel correlation mtx, the base station utilises the LS estimator followed by regularised ZF. The saddlepoint approximation comprises closed-form described quantities Lancho *et al.* (2020*b*). As a result, the evaluation procedure is extremely efficient. The average error probability tends to zero as $M \rightarrow \infty$ at finite blocklength. When MR is applied, however, the result converges to a positive integer. These results are indistinguishable from those obtained in the infinite-blocklength regime for Massive MIMO ergodic rates Björnson *et al.* (2018) and Sanguinetti *et al.* (2020).Numerical experiments can be used to evaluate the error probability feasible for limited values of M, as well as the impact of spatial correlation and pilot contamination. The fraction of UE placements metric, which is defined as the fraction of UE installations for which the per-link error

probability, averaged over small-scale fading and additive noise, is below a set threshold equivalent to network availability, can be used as a performance statistic Haenggi (2016). This amount is obtained in an asymptotic outage setting by describing the meta distribution of the signal to interference ratio (SIR) Haenggi (2016). The metadistribution of the generalised information density at limited blocklength is related to network availability. Martinez and i Fàbregas (2011).

For finite values of M, it is critical to account for spatial correlation in order to generate reasonable estimates of the error probability. Only by designating as many pilot symbols as the total number of UEs in the network and preventing pilot contamination can MMSE processing in UL and DL achieve network availability above 90%. When all cells employ the identical pilot sequences, network availability is just above 50%, however the shorter duration of the pilot sequences allows for a greater number of channel uses in the data phase. Even when pilot contamination is avoided, the network availability with MR precoding/combining remains below 50% for both UL and DL.

First, the finite-blocklength framework is constructed, which is utilised to investigate the impact of pilot contamination, spatial correlation, and the number of BS antennas on the error probability of a single-cell network with two UEs. The same is then implemented in a multicell multiuser context, as described in the paper fbl.

CHAPTER 2

RCUs ON THE PROBABILITY OF ERROR AT FINITE BLOCKLENGTH

wfe presents a numerical calculation of a finite-blocklength upper bound on the error probability based on the saddlepoint approximation. A simple situation is considered in which the received signal is a superposition of a scaled version of the intended signal and additive Gaussian noise. The analysis of a Massive MIMO network is done using this simple channel model.

2.1 RCUs for Deterministic and Random Channels

Consider a discrete complex-valued additive channel given by

$$v[k] = gq[k] + z[k], \quad k = 1, \ldots, n. \tag{2}$$

where $q[k] \in \mathbb{C} and v[k] \in \mathbb{C}$ are the input and output over channel use *k*, respectively, and *n* is the codeword length, $g \in \mathbb{C}$ is During the transmission of the n length codeword, the channel gain remains constant. The additive noise variables are distributed in i.i.d. $\mathcal{CN}(0,\, \sigma^2)$. Following assumptions are made:"

(a) The receiver does not know the channel gain *g* but has an estimate $\hat{g}$ of *g* which is treated as perfect.

(b) To determine the transmitted codeword $\underline{q} = [q[1], ..., q[n]]^T$, the receiver identifies the codeword $\tilde{\underline{q}}$ from the codebook $\mathcal{C}$ that is the closest to the received vector $\underline{v} = [v[1], ..., v[n]]^T \in \mathbb{C}^n$ in Euclidean distance sense."

$$\hat{\underline{q}} = \arg\min_{\tilde{\underline{q}} \in \mathcal{C}} \left\| \underline{v} - \hat{g}(\tilde{\underline{q}}) \right\|^2. \tag{3}$$

fbl A receiver working according to (3) is known as mismatched scaled nearest-neighbor (SNN) decoder Lapidoth and Shamai (1999). Note that it coincides with the optimal maximum likelihood decoder iff $\hat{g} = g$.

To find an upper bound on the error probability $\epsilon = \mathbb{P}[\underline{\tilde{q}} \neq \underline{q}]$ is achieved by the SNN decoding rule, a random-coding approach rgg. Gaussian random code ensemble is used where each codeword is drawn independently from a $\mathcal{CN}(0, \rho)$ distribution. (Note that this ensemble is not optimal at finite blocklength, not even if $\hat{g} = g$. It is, nonetheless, widely utilised to derive tractable statements and insights into the functioning of communication systems mas,fun, uni. This analysis can be extended to other ensembles, e.g., Östman *et al.* (2019)). Here, ρ is the average transmit power. The channel gain g in (2) can be modelled as a random or a deterministic variable. The former case is generally called as quasi static fading setting Biglieri *et al.* (1998).

Theorem 1: Assume that g $\in \mathbb{C}$ and $\hat{g} \in \mathbb{C}$ in (2) are deterministic. A coding scheme with $m = 2^b$ codewords of length *n* operating according to the mismatched SNN decoding rule (3), whose error probability ϵ is upper-bounded by

$$\epsilon = \mathbb{P}[\underline{\tilde{q}} \neq \underline{q}] \leq \mathbb{P}\left[\sum_{k=1}^{n} \imath_s(\mathbf{q}[\mathbf{k}], \mathbf{v}[\mathbf{k}]) + log(u) \leq log(m-1)\right] \tag{4}$$

for all *s* >0. Here, u is a random variable that is uniformly distributed over the interval[0,1] and $\imath_s(\mathbf{q}[\mathbf{k}], \mathbf{v}[\mathbf{k}])$)is the generalized information density, given by

$$\imath_s(\mathbf{q}[\mathbf{k}], \mathbf{v}[\mathbf{k}]) = -s|\mathbf{v}[\mathbf{k}] - \hat{g}\mathbf{q}[\mathbf{k}]|^2 + s\frac{|\mathbf{v}[\mathbf{k}]|^2}{1 + s\rho|\hat{g}|^2} + \log\left(1 + s\rho|\hat{g}|^2\right) \tag{5}$$

Assume now that g $\in \mathbb{C}$ and $\hat{g} \in \mathbb{C}$ in (2) are random variables drawn according to an arbitrary joint distribution. Then, for all $s > 0$, the error probability ϵ is upper-bounded by

$$\epsilon = \mathbb{P}[\underline{\tilde{q}} \neq \underline{q}] \leq \mathbb{E}_{\eth,\hat{\eth}}\left[\mathbb{P}\left[\sum_{k=1}^{n} \imath_s(\mathbf{q}[\mathbf{k}], \mathbf{v}[\mathbf{k}]) \leq \frac{log(m-1)}{u}\Big| g, \hat{g}\right]\right] \tag{6}$$

where the average is taken over the joint distribution of g and$\hat{g}$. If $\hat{g}$ is deterministic and g is a random variable ,the average in (6) is only taken over the distribution of gfbl. According to RCU_s bound introduced in Martinez and i Fàbregas (2011) for the case where g and $\hat{g}$ are deterministic. The upper bound for random g and $\hat{g}$ is calculated by

taking an expectation over the joint distribution of g and $\hat{g}$.

In the finite-blocklength domain, the probability of error can be expressed in terms of the probability that the empirical average of the generalised information density $\imath_s$ is less than the specified rate R= (logm)/n, whereas in infinite-blocklength regime, the outage probability is given by probability that the empirical average of the generalized mutual information $I_s = \mathbb{E}[\imath_s(q[1], v[1])]$ is less than the chosen rate R= (logm)/n Lapidoth and Shamai (1999). If g is known at the receiver, i.e.,$\hat{g} = g$, from the decoding rule (3) that $\epsilon \to 0$ when the SNR grows boundlessly, $\rho/\sigma^2 \to \infty$.

Lemma 1: If g = $\hat{g}$, then

$$\lim_{\rho/\sigma^2 \to \infty} \mathbb{P}\left[\sum_{k=1}^{n} \imath_s(\mathbf{q}[\mathbf{k}], \mathbf{v}[\mathbf{k}]) \leq \frac{log(m-1)}{u}\right] = 0 \tag{7}$$

The upper bounds in (4) and (6) involve computing the closed form of a tail probability that is unknown and must be computed numerically. They can be made tighter by optimising over the parameter s >0, which must be done numerically as well. All this numerical evaluation is computationally intensive, particularly low latency applications are dealt. This problem can be reduced by using a saddlepoint approximation.

2.2 Saddlepoint Approximation of RCUs bound

To numerically approximate (4) and (6) we need to perform a normal approximation on the probability term based on the Berry-Esseen central limit theorem because of evaluation of sum of tail probabilities [wfe,Ch. XVI.5]

$$\mathbb{P}\left[\sum_{k=1}^{n} \imath_s(\mathbf{q}[\mathbf{k}], \mathbf{v}[\mathbf{k}]) \leq \frac{log(m-1)}{u}\right] = Q\left(\frac{nI_s - log(m-1)}{\sqrt{nV_s}}\right) + o\left(\frac{1}{\sqrt{n}}\right) \tag{8}$$

where $I_s = \mathbb{E}[\imath_s(q[1], v[1])]$ is generalized mutual information Lapidoth and Shamai (1999),

$$V_s = \mathbb{E}[|\imath_s(q[1], v[1]) - I_s|^2] \tag{9}$$

is the variance of the information density computed with respect to the same distribution, typically referred to as channel dispersion Polyanskiy *et al.* (2010) and $o(1/\sqrt{n})$ is for terms that decay faster than $1/\sqrt{n}$ as n $\rightarrow \infty$. This normal approximation obtained by neglecting the $o(1/\sqrt{n})$ in (8) is accurate only when R= (logm)/n is close to I_s Lancho *et al.* (2020*b*). If we do not neglect the $o(1/\sqrt{n})$, it is called as refined normal approximation which is slightly beter than normal approximation because we are not ignoring any terms. However, to achieve the needed low error probabilities at SNR values of practical interest, we operate at speeds substantially lower than I_s in URLLC (Lancho *et al.* (2020*b*) Fig 3). The saddlepoint technique provides a more accurate estimate for all R values. The saddlepoint method's fundamental idea is to execute an exponential tilting on the random variables $\imath_s$(q[k],v[k]),k= 1,...,n, which brings their mean closer to the desired rate R. This ensures that a future application of the normal approximation produces modest mistakes[wfe, Ch. XVI.7] .

The approximations of the RCUs bound can be obtained by using saddlepoint method Scarlett *et al.* (2014), Lancho *et al.* (2020*b*). To derive the error probability, it is sufficient to check that the third central moment of $\imath_s(q[k], v[k])$ is bounded (which is the case in this situation), The presence of a saddlepoint approximation necessitates the more severe requirement that the third derivative of $-\zeta\imath_s(q[k], v[k])$ moment generating function (MGF) be in the neighbourhood of zero. It is deemed necessary that there exist two values $\underline{\zeta} < 0 < \bar{\zeta}$ such that

$$\sup_{\underline{\zeta}<\zeta<\bar{\zeta}} \frac{d^3}{d\zeta^3} \left| \mathbb{E}\left[e^{-\zeta\imath_s(q[k],v[k])}\right] \right| < \infty \tag{10}$$

where

$$\underline{\zeta} = -\frac{\sqrt{(\beta_B-\beta_A)^2+4\beta_A\beta_B(1-\nu)}+\beta_A-\beta_B}{2\beta_A\beta_B(1-\nu)} \tag{11}$$

$$\bar{\zeta} = -\frac{\sqrt{(\beta_B-\beta_A)^2+4\beta_A\beta_B(1-\nu)}-\beta_A+\beta_B}{2\beta_A\beta_B(1-\nu)} \tag{12}$$

$$\beta_A = s(\rho|g-\hat{g}|^2+\sigma^2) \tag{13}$$

$$\beta_B = \frac{s}{1+s\rho|\hat{g}|^2}(\rho|g|^2+\sigma^2) \tag{14}$$

$$\nu = \frac{s^2|\rho|g|^2 + \sigma^2 - g^*\hat{g}\rho|^2}{\beta_A\beta_B(1 + s\rho|\hat{g}|^2)} \tag{15}$$

fbl The saddlepoint approximation in Theorem 2 below depends on the cumulant generating function(CGF) of $\imath_s(q[k], v[k])$

$$\kappa(\zeta) = log\mathbb{E}[e^{-\zeta\imath_s(q[k],v[k])}] \tag{16}$$

and on its first derivative $\kappa\prime(\zeta)$ and second derivative $\kappa\prime\prime(\zeta)$. Closed form of these quantities for all $\zeta \in (\zeta, \bar{\zeta})$ are given by

$$\kappa(\zeta) = -\zeta log(1 + s\rho|\hat{g}^2|) - log(1 + (\beta_B - \beta_A)\zeta - \beta_A\beta_B(1 - \nu)\zeta^2) \tag{17}$$

$$\kappa\prime(\zeta) = -log(1 + s\rho|\hat{g}^2|) - \frac{(\beta_B - \beta_A) - 2\beta_A\beta_B(1 - \nu)\zeta}{1 + (\beta_B - \beta_A)\zeta - \beta_A\beta_B(1 - \nu)\zeta^2} \tag{18}$$

$$\kappa\prime\prime(\zeta) = \left[\frac{(\beta_B - \beta_A) - 2\beta_A\beta_B(1 - \nu)\zeta}{1 + (\beta_B - \beta_A)\zeta - \beta_A\beta_B(1 - \nu)\zeta^2}\right]^2 + \frac{2\beta_A\beta_B(1 - \nu)}{1 + (\beta_B - \beta_A)\zeta - \beta_A\beta_B(1 - \nu)\zeta^2} \tag{19}$$

$\kappa(\zeta)$ coincides with the Gallager's E_0 function for the mismatched case [Martinez and i Fàbregas (2011), Eq. (22)] $I_s = \kappa'(0)$. The critical rateR_s^{cr}(see [rgg, Eq. (5.6.30)]) is given by

$$R_s^{cr} = -\kappa'(1) \tag{20}$$

The saddlepoint expansion of the RCU_s bound (4) is given by

Theorem 2: Let $m = e^{nR}$ for some R >0, and let $\zeta \in (\zeta, \bar{\zeta})$ be the solution to the equation $R = \kappa'(\zeta)$ (from (18). If $\zeta \in$ [0,1], then $R_s^{cr} \leq R \leq I_s$ and

$$\mathbb{P}\left[\sum_{k=1}^{n} \imath_s(q[k], v[k]) \leq log\frac{e^{nR} - 1}{u} = e^{n[\kappa(\zeta)+\zeta R]}\left[\Psi_{n,\zeta}(\zeta) + \Psi_{n,\zeta}(1 - \zeta) + o(\frac{1}{\sqrt{n}})\right]\right] \tag{21}$$

where

$$\Psi_{n,\zeta}(u) \triangleq e^{n\frac{u^2}{2}\kappa''(\zeta)}Q\left(u\sqrt{n\kappa''(\zeta)}\right) \tag{22}$$

and $o(1/\sqrt{n})$ comprises terms that vanish faster than $1/\sqrt{n}$ and are uniform in ζ If ζ

>1, then R < R_s^{cr} and

$$\mathbb{P}\left[\sum_{k=1}^{n} \imath_s(q[k], v[k]) \leq log\frac{e^{nR}-1}{u} = e^{n[\kappa(1)+R]}\left[\tilde{\Psi}_n(1,1) + \tilde{\Psi}_{n,}(0,-1) + O(\frac{1}{\sqrt{n}})\right]\right] \tag{23}$$

where

$$\tilde{\Psi}_n(a_1, a_2) = e^{na_1[R_s^{cr}-R+\frac{\kappa''(1)}{2}]}Q\left(ua_1\sqrt{n\kappa''(1)} + a_2\frac{n(R_s^{cr}-R)}{\sqrt{n\kappa''(1)}}\right) \tag{24}$$

and $O(1/\sqrt{n})$comprises terms that are of order $1/\sqrt{n}$ and are uniform in ζ. If ζ <0, then R > I_s and

$$\mathbb{P}\left[\sum_{k=1}^{n} \imath_s(q[k], v[k]) \leq log\frac{e^{nR}-1}{u}\right] = 1-e^{n[\kappa(\zeta)+\zeta R]}\left[\Psi_{n,\zeta}(-\zeta) - \Psi_{n,\zeta}(1-\zeta) + o(\frac{1}{\sqrt{n}})\right] \tag{25}$$

fbl [Scarlett *et al.* (2014), App.E] [Lancho *et al.* (2020*b*), App. I].

Approximations obtained by ignoring the $o(1/\sqrt{n})$ terms and the $O(1/\sqrt{n})$ terms in (21), (23), and (25) are called as saddlepoint approximations. The exponential term on the right hand side of (21) and of (23) correspond to the Gallager's error exponent for the mismatch decoding scenario [Kaplan *et al.* (1991)]. The saddlepoint method's main idea is to isolate the Gallager error-exponent term, which determines the exponential decline of the probability of error as a function of blocklength, i.e., the exponential termin (21), (23), and (25). The Berry-Esseen central-limit theorem is then used to characterise solely the pre-exponential component, that is, the factor that multiplies the exponential term. wfe. Here, it can be noted that evaluating saddlepoint approximation for a ζ and its corresponding rate $R = \kappa(\zeta)$ warrants computational complexity same as that of the normal approximation as all quantities in (21), (23), and (25) are known is closed form.

The normal approximation and the saddlepoint approximation can both be tightened by doing an optimization over s, which is time consuming. Choosing a s that is optimal in an asymptotic regime is one technique to lessen the complexity of optimising s. Setting a value for s where generalised mutual information is maximised is one example.

In closed form, the corresponding value for s can be found. [Lapidoth and Shamai (1999) Eq. (64)].

2.3 Outage Probability

The error probability achievable for short blocklengths can be evaluated with bound (6) and we can check if outage probability is an accurate performance metric in Massive MIMO systems for URLLC apps. FA single-UE multiantenna system with a huge number M of antennas is explored for simplicity's sake. Between the UE and the BS array, there is a channel $\underline{h} \in \mathbb{C}^M$ and modelled as uncorrelated Rayleigh fading $\underline{h} \sim \mathcal{CN}(\underline{0}_M, \beta I_M)$ where β is large-scale fading gain mas. If the receiver has perfect CSI and the detection is done by MR combining, the input-output relationship for UL channels can be written as

$$v[k] = \frac{\underline{h}^H}{\|\underline{h}\|}\underline{h}q[k] + \frac{\underline{h}^H}{\|\underline{h}\|}\underline{z}'[k], \quad k = 1, \ldots, n \tag{26}$$

where $\underline{z}'[k] \sim \mathcal{CN}(\underline{0}_M, \sigma^2 I_M)$ is the thermal noise over the antenna array as a function of channel usage *k*. (26) can be transformed into (2) by setting $g = \frac{\underline{h}^H}{\|\underline{h}\|}\underline{h} = \|\underline{h}\| \& z[k] = \frac{\underline{h}^H}{\|\underline{h}\|}\underline{z}'[k] \sim \mathcal{CN}(0, \sigma^2)$. We have $\hat{g} = g = \|\underline{h}\|$ since h is perfectly known at the receiver. $\hat{g} = g = \|\underline{h}\|$. The probability term in (6) in the limit $n \to \infty$ is equal to 1 once the parameter s has been tuned if $log(1 + \rho|g|^2/\sigma^2) < R$ and 0 otherwise. As a result, the bound in (6) approaches the outage probability

$$\mathbb{P}\left[log\left(1 + \frac{\rho g^2}{\sigma^2}\right) < R\right] \tag{27}$$

Here, the probability is evaluated with respect to the random variable $g = \|\underline{h}\|$.

CHAPTER 3

SCENARIO FOR SINGLE-CELL TWO-UE MASSIVE MIMO

A single-cell network is examined, in which the BS has M antennas and serves K= 2 single-antenna UEs. $\underline{h}_i \in \mathbb{C}^M$ is the channel vector between the BS and UE i for i= 1,2. A correlated Rayleigh fading model $\underline{h}_i \sim \mathcal{CN}(\mathbf{0}_M, \mathbf{R}_i)$ is regarded constant for the duration of a codeword transmission. The normalized trace $\beta_i = tr(\mathbf{R}_i)/M$ determines the average large-scale fading between the BS and the UEi, while the eigen structure of $\mathbf{R}_i$ explains the spatial channel correlation between the two. [mas Sec.2.2]. It is assumed that $\mathbf{R}_1$ and $\mathbf{R}_2$ are known at the BS. Sanguinetti *et al.* (2020), Björnson *et al.* (2016) describe practical estimation methods.

3.1 Uplink transmission

The standard time division duplex (TDD) Massive MIMO technique is used, with UL and DL transmissions each receiving n channel uses, divided into n_p channel uses for UL pilots, $n_u l$ channel uses for UL data, and $n_d l = n - n_u l$ channel uses for DL data. The n_p length pilot sequence $\phi_i \in \mathbb{C}^{n_p}$ with $\phi_i^H \phi_i = n_p$ is used by UE i for channel estimation. The elements of ϕ_i are transmitted over n_p channel uses and are scaled by the square root of the pilot power $\sqrt{\rho^{ul}}$. After pilot sequences are transmitted by UEs, received pilot signal $\mathbf{Y}^{pilot} \in \mathbb{C}^{M \times n_p}$ is

$$\mathbf{Y}^{pilot} = \sqrt{\rho^{ul}} \underline{h}_1 \underline{\phi}_1^H + \sqrt{\rho^{ul}} \underline{h}_2 \underline{\phi}_2^H + \mathbf{Z}^{pilot} \tag{28}$$

where $\mathbf{Z}^{pilot} \in \mathbb{C}^{M \times n_p}$ is the additive noise with independent and identical distributed elements as $\mathcal{CN}(0, \sigma_{ul}^2)$. Assuming that $\mathbf{R}_1$ and $\mathbf{R}_2$ are well-known at the BS, and h_i's

MMSE estimate is [mas]

$$\hat{\underline{h}}_i = \sqrt{\rho^{ul} n_p} \mathbf{R}_i \mathbf{Q}_i^{-1} (\mathbf{Y}^{pilot} \underline{\phi}_i) \tag{29}$$

for i = 1,2 with

$$\mathbf{Q}_i = \rho^{ul} \mathbf{R}_1 \underline{\phi}_1^H \underline{\phi}_i + \rho^{ul} \mathbf{R}_2 \underline{\phi}_2^H \underline{\phi}_i + \sigma_{ul}^2 \mathbf{I}_M \tag{30}$$

The MMSE estimate $\hat{\underline{h}}_i$ and the estimation error $\tilde{\underline{h}}_i = \underline{h}_i - \hat{\underline{h}}_i$ are independent random vectors, distributed as $\hat{\underline{h}}_i \sim \mathcal{CN}(\mathbf{0}, \mathbf{\Phi}_i)$ and $\tilde{\underline{h}}_i \sim \mathcal{CN}(\mathbf{0}, \mathbf{R}_i - \mathbf{\Phi}_i)$, consecutively, $\mathbf{\Phi}_i = \rho^{ul} n_p \mathbf{R}_i \mathbf{Q}_i^{-1} \mathbf{R}_i$.

If $\phi_1^H \phi_2 = 0$, i.e. There is no interference if the two UEs use orthogonal pilot sequences, but if they use the same pilot sequence ($phi_1 = phi_2$), they interfere, which is known as pilot contamination and has two primary repercussions in the channel estimation process. [masSec. 3.2.2].The first is a reduction in estimating quality, while the second is a correlation between the estimations $\hat{\underline{h}}_1$ and $\hat{\underline{h}}_2$. If $\phi_1 = \phi_2$, then $\mathbf{Y}^{pilot}\phi_1 = \mathbf{Y}^{pilot}\phi_2$ and $\mathbf{Q}_1 = \mathbf{Q}_2 = \mathbf{Q}$ with $\mathbf{Q} = \rho^{ul} n_p \mathbf{R}_1 + \rho^{ul} n_p \mathbf{R}_2 + \sigma_{ul}^2 \mathbf{I}_M$. $\hat{\underline{h}}_2$ can be denoted by $\mathbf{R}_2 \mathbf{R}_1^{-1} \hat{\underline{h}}_1$ on condition that $\mathbf{R}_1$ is invertible. This indicates that the estimates are correlated, and the cross-correlation matrix is $\mathbb{E}\left[\hat{\underline{h}}_1 \hat{\underline{h}}_2^H\right] = \mathbf{\Upsilon}_{12} = \rho^{ul} n_p \mathbf{R}_1 \mathbf{Q}^{-1} \mathbf{R}_2$.This holds true even if the underlying channels are statistically independent with $\mathbb{E}\left[\underline{h}_1 \underline{h}_2^H\right] = \mathbf{0}_M$. If $\mathbf{R}_i = \beta_i \mathbf{I}_M$ i.e. if no spatial correlation is present, then the channel estimates are linearly dependent meaning they are identical up to a scaling factor.

The received complex BB signal $\underline{r}^{ul}[k] \in \mathbb{C}^M$ over an arbitrary channel usage *k* during the UL data transmission where $k = 1, \ldots, n_{ul}$ is given by

$$\underline{r}^{ul}[k] = \underline{h}_1 x_1^{ul}[k] + \underline{h}_2 x_2^{ul}[k] + \underline{h}^{ul}[k] \tag{31}$$

where $x_i^{ul}[k] \sim \mathcal{CN}(0, \rho^{ul})$ is the signal that carries information (When the elements of each codeword are picked independently from a Gaussian random code ensemble, the error probability is calculated from $\mathcal{CN}(0, \rho^{ul})$ distribution) transmitted by UE *i* with average UL transmit power as ρ^{ul} and $\underline{h}^{ul}[k]\mathcal{CN}(\mathbf{0}, \sigma_{ul}^2 \mathbf{I}_M)$ is independent additive noise. The signal $x_1^{ul}[k]$ is detected by the BS using the combining vector $\underline{u}_1 \in \mathbb{C}^M$ to

get

$$y_1^{ul}[k] = \underline{u}_1^H \underline{r}^{ul}[k] = \underline{u}_1^H \underline{h}_1 x_1^{ul}[k] + \underline{u}_1^H \underline{h}_2 x_2^{ul}[k] + \underline{u}_1^H \underline{z}^{ul}[k] \tag{32}$$

(32) is similar to (2) with $v[k] = y_1^{ul}[k]$, $q[k] = x_1^{ul}[k]$, $g = \underline{u}_1^H \underline{h}_1$ and $z[k] = \underline{u}_1^H \underline{h}_2 x_2^{ul}[k] + \underline{u}_1^H \underline{z}^{ul}[k]$. Given $\{\underline{h}_1, \underline{u}_1, \underline{h}_2\}$, the random variables $z[k]$ $k = 1, \ldots, n_{ul}$ are conditionally i.i.d. and $z[k] \sim \mathcal{CN}(0, \sigma^2)$ with $\sigma^2 = \rho^{ul} |\underline{u}_1^H \underline{h}_2|^2 + \|\underline{u}_1\|^2 \sigma_{ul}^2$.

It is assumed that BS treats the obtained noisy channel estimate $\hat{\underline{h}}_1$ as perfect. To retrieve the transmitted codeword (drawn from a codebook $\mathcal{C}^{ul}$), BS performs mismatched SNN decoding with $\hat{g} = \underline{u}_1^H \hat{\underline{h}}_1$. Particularly, the estimated codeword $\hat{\underline{x}}_1^{ul}$ is given by

$$\hat{\underline{x}}_1^{ul} = \underset{\tilde{\underline{x}}_1^{ul} \in \mathcal{C}^{ul}}{arg\ min} \|\underline{y}_1^{ul} - (\underline{u}_1^H \hat{\underline{h}}_1) \tilde{\underline{x}}_1^{ul}\|^2 \tag{33}$$

with $\underline{y}_1^{ul} = \left[y_1^{ul}[1], \ldots, y_1^{ul}[n_{ul}]\right]^T$ and $\tilde{\underline{x}}_1^{ul} = \left[\tilde{x}_1^{ul}[1], \ldots, \tilde{x}_1^{ul}[n_{ul}]\right]^T$. Eq. (4) establishes a limit on the conditional error probability for UE 1 given g and $\hat{g}$. We need to take an expectation over g to determine the average error probability $g = \underline{u}_1^H \underline{h}_1$, $\hat{g} = \underline{u}_1^H \hat{\underline{h}}_1$ and $\sigma^2 = \rho^{ul} |\underline{u}_1^H \underline{h}_2|^2 + \|\underline{u}_1\|^2 \sigma_{ul}^2$, which gives

$$\epsilon_1^{ul} \leq \mathbb{E}\left[\mathbb{P}\left[\sum_{k=1}^{n_{ul}} \imath_s(y_1^{ul}[k], x_1^{ul}[k]) \leq \frac{log(m-1)}{u} \Big| g, \hat{g}, \sigma^2\right]\right] \tag{34}$$

The saddlepoint approximation stated in Theorem 2 can be applied as it is to compute the conditional probability in (34) efficiently. The average error probability for UE 2 can be computed in similar manner. The combining vector u_1 is selected at the BS based on the channel estimates $\hat{\underline{h}}_1$ and $\hat{\underline{h}}_2$. The most straightforward option would be to use MR combining which is $\underline{u}_1^{MR} = \hat{\underline{h}}_1 / M$. MMSE, which is more computationally intensive, is another option.

$$\underline{u}_1^{MMSE} = \left(\sum_{i=1}^{2} \hat{\underline{h}}_i \hat{\underline{h}}_i^H + Z\right)^{-1} \hat{\underline{h}}_1 \tag{35}$$

where $Z = \sum_{i=1}^{2} \Phi_i + \frac{\sigma_{ul}^2}{\rho^{ul}} I_M$.

3.2 Downlink transmission

The BS transmits to UE I with I = 1,2 using the precoding vector. The precoding vector determines the transmission's spatial directivity and also ensures that the normalisation $\mathbb{E}[\|\underline{w}_i\|^2] = 1$ is met. . The received signal at UE 1 $y_1^{dl}[k] \in \mathbb{C}$ over channel use k during DL data transmission, where *k* = $1, \ldots, n_{dl}$ is given by

$$y_1^{dl}[k] = \underline{h}_1^H \underline{w}_1 x_1^{dl}[k] + \underline{h}_1^H \underline{w}_2 x_2^{dl}[k] + z^{dl}[k] \tag{36}$$

where $x_i^{dl}[k] \sim \mathcal{CN}(0, \rho^{dl})$ is the data signal for UE *i* and $x_1^{dl}[k] \sim \mathcal{CN}(0, \sigma_{dl}^2)$ is the receiver noise at UE 1. Again, (36) is similar to (2) with $v[k] = y_1^{dl}[k]$, $q[k] = x_1^{dl}[k], g = \underline{h}_1^H \underline{w}_1$ and $z[k] = h_1^H w_2 x_2^{dl}[k] + z^{dl}[k]$. Given $\{\underline{h}_1, \underline{w}_1, \underline{w}_2\}$, the random variables $z[k] : k = 1, \ldots, n_{dl}$ are conditionally i.i.d. and $z[k] \sim \mathcal{CN}(0, \sigma^2)$ with $\sigma^2 = \rho^{dl}|\underline{h}_1^H \underline{w}_2|^2 + \sigma_{dl}^2$.

The UE does not know the precoded channel because there are no pilots to be broadcast in the DL. $g = \underline{h}_1^H \underline{w}_1$ in (36), UE, on the other hand, is presumed to have its expected value $\mathbb{E}[h_1^H w_]$ The mismatched SNN decoding is performed using this expected value. We use $\hat{g} = \mathbb{E}[\underline{h}_1^H \underline{w}_1]$ and

$$\underline{\hat{x}}_1^{dl} = \underset{\tilde{x}_1^{dl} \in \mathcal{C}^{dl}}{arg\ min} \|\underline{y}_1^{dl} - \hat{g}\underline{\tilde{x}}_1^{dl}\|^2 \tag{37}$$

with $\underline{y}_1^{dl} = \left[y_1^{dl}[1], \ldots, y_1^{dl}[n_{dl}]\right]^T$ and $\underline{\tilde{x}}_1^{dl} = \left[\tilde{x}_1^{dl}[1], \ldots, \tilde{x}_1^{ul}[n_{dl}]\right]^T$. HIn order for this option to operate well, channel hardening is required.[mas Sec 2.5.1]. Since $\hat{g} = \mathbb{E}[\underline{h}_1^H \underline{w}_1]$ is deterministic, The following formula can be used to compute the error probability at UE 1 in the DL:

$$\epsilon_1^{dl} \leq \mathbb{E}\left[\mathbb{P}\left[\sum_{k=1}^{n_{dl}} \imath_s(y_1^{dl}[k], x_1^{dl}[k]) \leq \frac{log(m-1)}{u} \Big| g, \sigma^2\right]\right] \tag{38}$$

The saddlepoint approximation mentioned in Theorem 2 may be used to efficiently compute the conditional probability in (38) in the same way it can be used to compute the conditional probability in (34). The upper bound (38), like the UL, applies to

any precoder vector chosen based on the channel estimates given at the BS. Different precoders produce different tradeoffs in terms of the error probability achieved at the UEs. A common heuristic comes from UL-DL duality [mas Sec. 4.3.2] This implies that the precoding vectors w_i should be chosen as a function of the combining vectors as $\underline{w}_i = u_i/\sqrt{\mathbb{E}[\|\underline{u}_i\|^2]}$. If the MR precoding technique is selected $\underline{u}_i = \underline{u}_i^{MR}$ and $\underline{u}_i = \underline{u}_i^{MMSE}$ if MMSE precoding scheme is chosen.

The finite blocklength bound stated in Theorem 1 is used to investigate the impact of imperfect CSI, pilot contamination, and spatial correlation for both UL and DL. The setting as mentioned in the paperfbl is considered. K= 2UEs are within a square area of 75m$\times$75m is considered with the BS at the center of the square. The BS is equipped with a horizontal uniform linear array (ULA) with antenna elements separated by half a wavelength. For a circular array of N=8 antenna elements evenly spaced on a circle of radius $R = Nd/2\pi$. This radius is chosen to obtain approximately half a wavelength spacing of the elements, equivalent to that used for the linear array. For Unifrom circular array (UCA), the nominal angle considered is 40 degrees and ASD (power azimuth spectrum standard deviation)is 25 degrees is used to plot network availability with respect to target probability of error. Because the antennas and UEs are in the same horizontal plane, learning the directivity requires only an azimuth angle. IScatterers are considered to be evenly dispersed throughout the angular interval $[\varphi - \triangle, \varphi + \triangle]$ where φ is the nominal angle of arrival (AoA) of UE *i* and $\triangle$ s the angular spread. Hence, the $(m_1, m_2)^{th}$ element of R_i is equal to [mas, Sec. 2.6]

$$[R_i]_{m_1,m_2} = \frac{\beta_i}{2\triangle} \int_{-\triangle}^{\triangle} e^{j\pi(m_1 - m_2)sin(\varphi_i + \bar{\varphi})} d\bar{\varphi} \tag{39}$$

$\triangle = 25^\circ$ is assumed and large-scale fading coefficient, measured in dB is

$$\beta_i = -35.3 - 37.6log_{10}\left(\frac{d_i}{1m}\right) \tag{40}$$

distance between UE i and BS d_i. Parameters considered are receiver noise power of -94dBm in both uplink and downlink at both UEs and BS. The Uplink and Downlink transmit powers are equal and equal to 10mW and number of channel uses are 300 and

160 information bits are to be conveyed. These parameters are in agreement with the stringent low-latency setups described in [ser].

The error probability of MR combining in the UL is found to be higher than that of MR precoding in the DL. By comparing the input output relations in (32) and (36) for the situation of perfect CSI at both BS and UEs, this occurrence can be explained. When the desired signal fades deeply, the UL interference remains unaffected, however the DL interference decreases. As a result, UL has a higher mistake probability than DL. The same logic holds true for both pilot contamination and faulty CSI. This occurence does not occur when MMSE combining/precoding is used. In contrast, because DL decoding relies on channel hardening, the DL performs slightly worse than the UL when using MMSE precoding.

$$\eta = \mathbb{P}\epsilon \leq \epsilon_{target}] \tag{41}$$

η shows the probability that the target error probability ϵ_{target} s attained on a link between a BS and randomly positioned UE in the presence of randomly positioned interfering UEs (just one in this case). TGiven the UEs location, the network availability is estimated with regard to random UE locations, whereas the error probability ϵ is averaged with respect to small-scale fading and additive noise. Network availability with and without pilot contamination is considered.

3.3 Error Probability as $M \to \infty$

The interference generated by pilot contamination restricts the spectral efficiency of Massive MIMO in the large blocklength ergodic configuration for spatially uncorrelated Rayleigh fading channels as $M \to \infty$ and the number of UEs *K* is fixed, for both MR and MMSE combining/precoding Marzetta (2010), Hoydis *et al.* (2011). However, when the spatial correlation displayed by practically relevant channels is taken into account, Björnson *et al.* (2018) shows that Massive MIMO with MMSE combining/precoding is not asymptotically restricted by pilot contamination.

When $M \to \infty$ and K = 2 (simple case), a similar conclusion applies for the average error probability in the finite blocklength regime. As $M \to \infty$, the error probability vanishes in the presence of spatial correlation when MMSE combining is used. Following two assumptions are made in fbl:

Assumption 1: For i = 1,2, $\liminf_M \frac{1}{M} tr(R_i) > 0 \; and \; \limsup_M \|R_i\|_2 < \infty$

Assumption 2: For $(\lambda_1, \lambda_2) \in \mathbb{R}^2$ and i = 1,2,

$$\liminf_M \inf_{\{(\boldsymbol{\lambda_1}, \boldsymbol{\lambda_2}) : \lambda_i = 1\}} \frac{1}{M} \|\lambda_1 \mathbf{R}_1 + \lambda_2 \mathbf{R}_2\|_F^2 > 0. \tag{42}$$

Assumption 1's first condition means that the array collects a quantity of signal energy proportional to M. The second criterion entails that the enhanced signal energy is dispersed across a large number of spatial dimensions, i.e., the rank of R_i must be proportional to M Björnson *et al.* (2018). In the asymptotic analysis of Massive MIMO, these two requirements are frequently mentioned Hoydis *et al.* (2011). Assumption 2 needs asymptotically linear independence for R_1 and R_2. Sanguinetti *et al.* (2020).

If there is no pilot contamination, the likelihood of mistake vanishes as $M \to \infty$ with MR combining, as demonstrated in in below Theorem 3. i.e. if the two UEs transmit orthogonal pilot sequences. If there is pilot contamination, i.e. if they have the same pilot sequence, it converges to a positive constant.

Theorem 3: Let $c > 0$ be a positive realvalued scalar. If MR combining is used with $u_1^{MR} = \frac{1}{M} \hat{h}_1$, then under Assumption 1,

$$\lim_{M \to \infty} \epsilon_1^{ul} = 0, \; if \; \phi_1^H \phi_2 = 0, \tag{43}$$

$$\lim_{M \to \infty} \epsilon_1^{ul} = c, \; if \; \phi_1 = \phi_2, \tag{44}$$

fbl

Even in the presence of pilot contamination, the error probability vanishes as $M \to \infty$ with MMSE combining, as stated in Theorem 4.

Theorem 4: If MMSE combining is used with u_1^{MMSE} given by (35), then under

Assumption 1 and Assumption 2, the average error probability ϵ_1^{ul} goes to zero as $M \to \infty$ both when $\phi_1^H \phi_2 = 0$ and when $\phi_1 = \phi_2$. fbl

When the two UEs transmit at the same power, are at the same distance from the BS, and use the same pilot sequence, the UL error probability is numerically evaluated to validate the asymptotic analysis provided by Theorems 3 and 4 and to quantify the impact of pilot contamination for values of M of practical interest.

CHAPTER 4

MASSIVE MIMO NETWORK

The case will now be a Massive MIMO network with L cells, each with a BS with M antennas and K UEs. The channel between UE *i* in cell *l* and the BS in cell *j* is $h_{li}^{j} \sim \mathcal{CN}(0_M, R_{li}^{j})$. The n_p length pilot sequence of UE *i* in cell *j* is denoted by the vector $\phi_{ji} \in \mathbb{C}^{n_p}$ and satisfies $\|\phi_{ji}\|^2 = n_p$. It is assumed that a cell's K UEs employ mutually orthogonal pilot sequences, and that these pilot sequences are reused in 1/f of the L cells with $n_p = Kf$. The MMSE estimator is used to estimate the channel vectors. [mas, Sec 3.2].

4.1 Uplink Transmission

The data signal from UE i' in cell *l* at any point in time *k* is denoted by $x_{li'}^{j}[k] \sim \mathcal{CN}(0, \rho^{ul})$ where ρ^{ul} is transmit power. For the detection of $x_{ji}[k]$, BS *j* selects precoding vector $\underline{v}_{ji} \in \mathbb{C}^M$, which is multiplied with the received signal $\underline{y}_j[k]$ to get

$$r_{ji}[k] = \underline{v}_{ji}^H \underline{y}_j[k] = \overbrace{\underbrace{\underline{v}_{ji}^H \underline{h}_{ji}^j x_{ji}[k]}_{\text{Desired signal}}}^{gq[k]} + \overbrace{\underbrace{\sum_{i'=1, i' \neq i}^{K} \underline{v}_{ji}^H \underline{h}_{ji'}^j x_{ji'}[k]}_{\text{Intra-cell Interference}}}^{z[k]} + \overbrace{\underbrace{\sum_{l=1, l \neq j}^{L} \sum_{i'=1}^{K} \underline{v}_{ji}^H \underline{h}_{li'}^j x_{li'}[k]}_{\text{Inter-cell Interference}}}^{z[k]} + \overbrace{\underbrace{\underline{v}_{ji}^H \underline{z}_j[k]}_{\text{Noise}}}^{z[k]} \tag{45}$$

for $k = 1, \ldots, n_p$. (45) can be put in the same form as (2) if we set $v[k] = r_{ji}[k],\ q[k] = x_{ji}[k], \quad g = \underline{v}_{ji}^H \underline{h}_{ji}^j,\ \hat{g} = \underline{v}_{ji}^H \hat{\underline{h}}_{ji}^j \quad and\ z[k] = \sum_{i'=1, i' \neq i}^{K} \underline{v}_{ji}^H \underline{h}_{ji'}^j x_{ji'}[k] + \sum_{l=1, l \neq j}^{L} \sum_{i'=1}^{K} \underline{v}_{ji}^H \underline{h}_{li'}^j x_{li'}[k] + \underline{v}_{ji}^H \underline{z}_j[k]$. The random variables $z[k] : k = 1, \ldots, n_{ul}$

are iid given all channels and combining vectors and $z[k] \sim \mathcal{CN}(0, \sigma^2)$ with $\sigma^2 = \sigma_{ul}^2 \|\underline{v}_{ji}\|^2 + \rho^{ul} \sum_{i'=1, i' \neq i}^{K} |\underline{v}_{ji}^H \underline{h}_{ji'}^j|^2 + \rho^{ul} \sum_{l=1, l \neq j}^{L} \sum_{i'=1}^{K} |\underline{v}_{ji}^H \underline{h}_{li'}^j|^2$. Theorem (1) is then used to calculate an upper bound on the error probability ϵ_{ji}^{ul} , which is subsequently averaged over $g,\ \hat{g},\ \sigma^2$. This bound is true for any v_{ji}. value.

4.2 Downlink Transmission

The Downlink signal $x_j[k]$ is transmitted by the BS in cell j $x_j[k] = \sum_{ji'=1}^{K} \underline{w}_{ji'} x_{ji'}[k]$, where $x_{ji'}[k] \sim \mathcal{CN}(0, \rho^{dl})$ is the Downlink data signal planned for UE i' in cell *j* over the time index *k*, assigned to a combining vector $\underline{w}_{ji'} \in \mathbb{C}^M$ which satisfies $\|\underline{w}_{ji'}\|^2 = 1$ and ρ^{dl} is the power transmitted. The received signal $y_{ji}[k] \in \mathbb{C}$ for $k = 1, \ldots, n_{dl}$ at UE *i* in cell *j* is given by

$$y_{ji}[k] = v_{ji}^H y_j[k] = \overbrace{\underbrace{(\underline{h}_{ji}^j)^H \underline{w}_{ji} x_{ji}[k]}_{\text{Desired signal}}}^{gq[k]} + \overbrace{\underbrace{\sum_{i'=1, i' \neq i}^{K} (\underline{h}_{ji}^j)^H \underline{w}_{ji'} x_{ji'}[k]}_{\text{Intra-cell Interference}}}^{z[k]} + \overbrace{\underbrace{\sum_{l=1, l \neq j}^{L} \sum_{i'=1}^{K} (\underline{h}_{ji}^l)^H \underline{w}_{li'} x_{li'}[k]}_{\text{Inter-cell Interference}}}^{z[k]} + \overbrace{\underbrace{z_{ji}[k]}_{\text{Noise}}}^{z[k]} \tag{46}$$

where $z_{ji}[k] \sim \mathcal{CN}(0, \sigma_{dl}^2)$ is the receiver noise. The desired signal to UE *i* in cell *j* transmits over the combined channel $g_{ji} = (\underline{h}_{ji}^j)^H \underline{w}_{ji}$. The UE does not know g_{ji} and relies on channel hardening to estimate it with its mean value $\mathbb{E}[g_{ji}] = \mathbb{E}[(\underline{h}_{ji}^j)^H \underline{w}_{ji}]$. Similar to Uplink case, (46) can be put in the same form as (2) if we set $v[k] = y_{ji}[k],\ q[k] = x_{ji}[k],\ g = (\underline{h}_{ji}^j)^H \underline{w}_{ji},\ \hat{g} = \mathbb{E}[(\underline{h}_{ji}^j)^H \underline{w}_{ji}]$ *and* $z[k] = \sum_{i'=1, i' \neq i}^{K} (\underline{h}_{ji}^j)^H \underline{w}_{ji'} x_{ji'}[k] + \sum_{l=1, l \neq j}^{L} \sum_{i'=1}^{K} (\underline{h}_{ji}^l)^H \underline{w}_{li'} x_{li'}[k] + z_{ji}[k]$. Given combining vectors and all channels, the random variables $z[k] : k = 1, \ldots, n_{dl}$ are conditionally i.i.d. and $z[k] \sim \mathcal{CN}(0, \sigma^2)$ with $\sigma^2 = \sigma_{dl}^2 + \rho^{ul} \sum_{i'=1, i' \neq i}^{K} |(\underline{h}_{ji}^j)^H \underline{w}_{ji'}|^2 + \rho^{ul} \sum_{l=1, l \neq j}^{L} \sum_{i'=1}^{K} |(\underline{h}_{ji}^j)^H \underline{w}_{ji'}|^2$. Theorem (1) is then used to calculate an upper bound on the error probability ϵ_{ji}^{dl}, which is subsequently averaged over g and σ^2. This constraint holds for any $\underline{w}_{ji}$. value.

CHAPTER 5

Simulation results

5.1 RCUs bound on the Error probability

In 5.1a, the probability of error as a function of number of antennas M is plotted with a fixed SNR of 1 dB. Other parameters are taken as- rate is 0.6 bits per channel use, codeword length is 100. In addition to the normal approximation shown in the paper, I also implemented refined normal approximation and also fig c. From the figure we can observe that outage capacity is followed by normal approximation or even refined normal approximation in that matter for only small values of number of antennas. The saddlepoint approximation provides a better bound for all values of M as observed in the figure.

In 5.1b, the probability of error as a function of number of antennas M without fixed SNR is plotted so that average SNR increases as number of antennas increases. Transmit power is fixed at -24dBm. Here, it can be observed that the saddlepoint approximation provide better bounds than normal approximation or refined normal approximation for upto probability of error of 10^{-4}.

In 5.1c, the probability of error as a function of rate is plotted. Parameters are blocklength is 128, with SNR -24dB and number of antennas are 200. In this plot, we can clearly observe that for short block lengths, the outage capacity moves away from theoretical Shannon channel capacity. So, for short block length codes, we cannot take outage capacity as a benchmark. In presence of imperfect CSI, these approximations become even more questionable. The nonasymptotic bound (6), which may be efficiently computed using the saddlepoint approximation, can be used to completely eliminate this difficulty. How the simple input output relation (2) may be utilised to analyse practical Massive MIMO networks with faulty CSI, spatial correlation among antennas, pilot contamination, and both inter-cell and intra-cell interference.

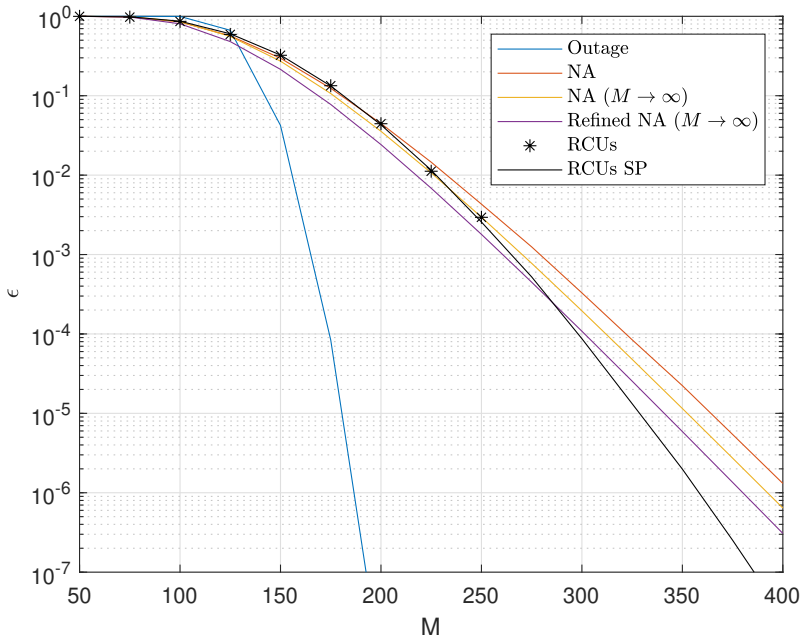

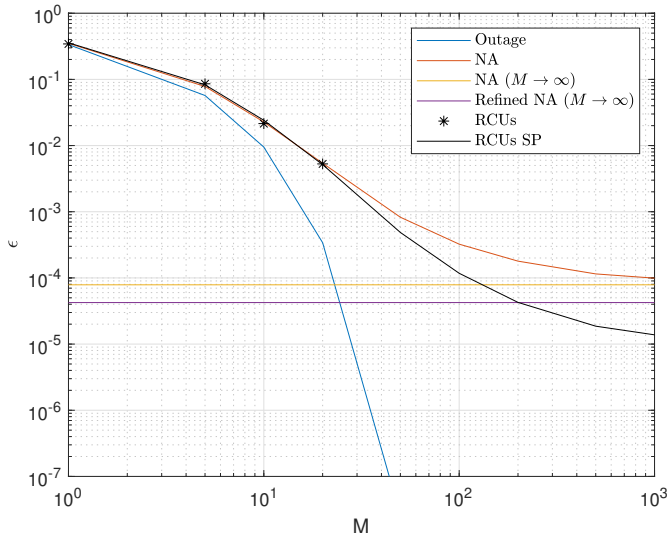

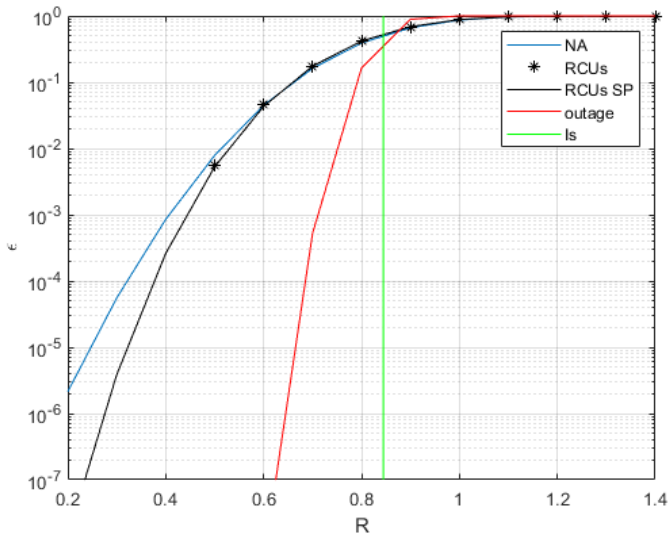

Fig. 5.1: Average error probability in the UL of a single UE multiantenna system when$\hat{g} = g = \|h\|$ $with$ $h \sim \mathcal{CN}(0_M, \beta I_M)$, n=100,R=0.6 bits per channel use. (a)ϵ vs M (Fixed average received SNR= 1 dB). (b) ϵ vs M (Fixed transmit power ρ= 24 dBm). (c) ϵ vs R

5.2 RCUs bound on the Error probability for the case of Single Cell 2 UE MIMO

Fig 5.2 a,b show the Uplink and Downlink error probability ϵ of UE 1 with MR and MMSE combining, with and without Pilot contamination when M= 100 and 200. The nominal angle of UE 1 is fixed at $\varphi_1 = 30^\circ$ while the angle of UE 2 varies from 0° to 65°. $d_1 = d_2 = 36.4m$ and $\beta_1 = \beta_2 = -94dB$. Even if pilot contamination influences channel estimates, a low error probability can be attained if the UEs are properly separated in the angle domain. When compared to MR precoding, MMSE combining/precoding achieves a significantly reduced error probability for a given angle separation. These findings are consistent with those published in the asymptotic regime for large packet sizes in Sanguinetti *et al.* (2020).

Fig 5.3 shows network availability η in Uplink and Downlink with both MR and MMSE when M = 100 and other parameters are same as that of fig 5.2.

Fig 5.3: Regardless of the processing scheme, network availability is lowered when there is pilot contamination. When orthogonal pilot sequences are used, MR operates better in the Downlink compared to Uplink (similar reasoning in 5.2 above), but if there is pilot contamination, Uplink performance is better when the UE depends on channel hardening and slightly worse when UE has access to perfect CSI. The correlation matrix may have a low rank due to the random UE placements. This has an impact on channel hardening and, as a result, DL performance suffers. Because the DL relies on channel hardening, the UL is always superior to the DL when it comes to MMSE processing.

In Fig5.4(a), average error probability as a function of *M* with MR and MMSE is shown. It is assumed that the nominal angles are $\varphi_1 = 30^\circ$ and $\varphi_1 = 40^\circ$. Because the angle between the two UEs is less, pilot contamination is likely to have a substantial impact on the error probability. Parameters are similar to fig5.2. in the presence of pilot contamination, the error probability with MR converges to a nonzero constant as M increases, whereas the error probability with MMSE converges to 0 as $M \to \infty$ 5.4. Error probability with respect to number of antennas are simulated for UCA case also,

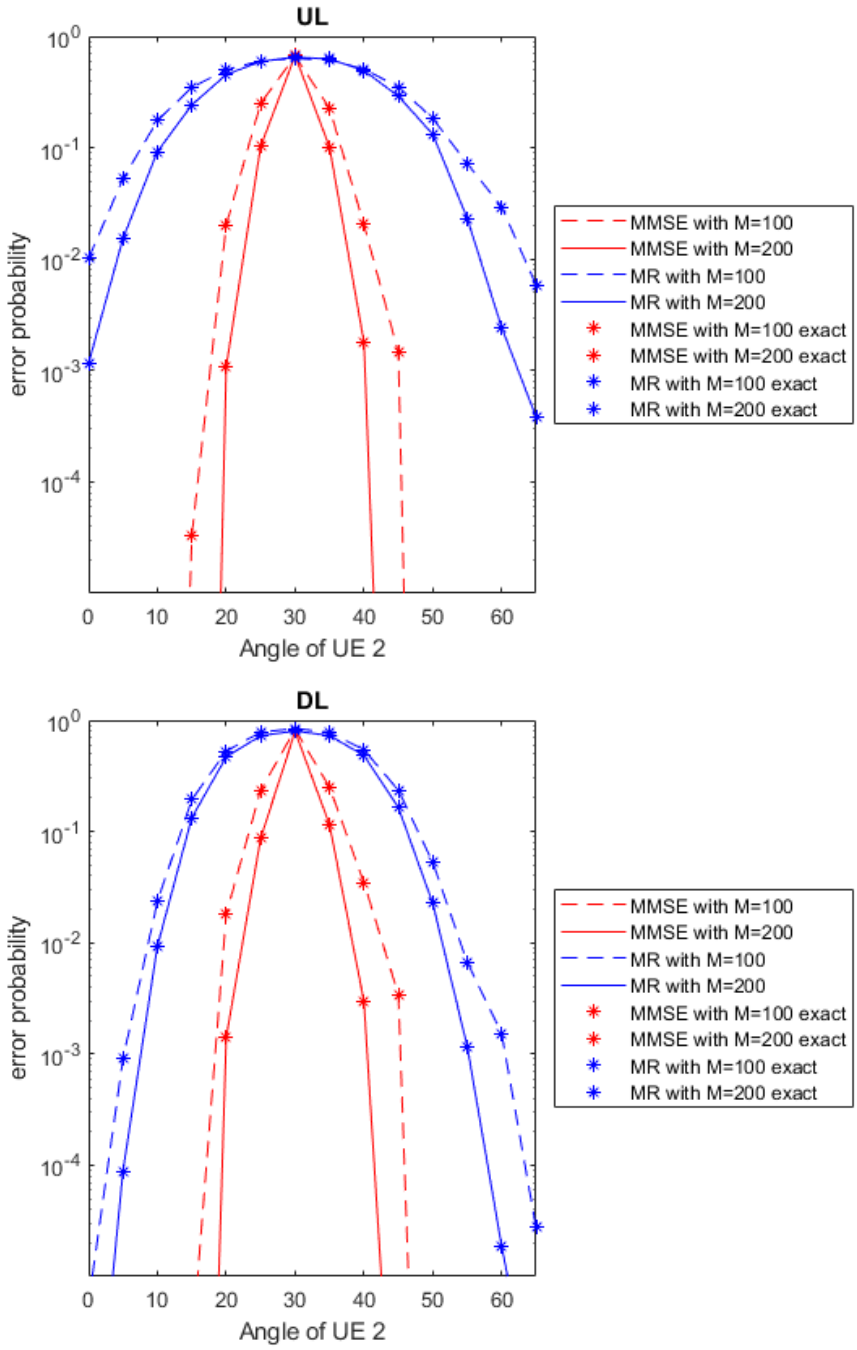

Fig. 5.2: Average error probability ϵ or UE1 versus the nominal angle of UE2 with pilot contamination. The curves are obtained using the saddlepoint approximation, the stars indicate the values of the RCUs bound, computed directly via (6).(a) Uplink transmission. (b) Downlink transmission.

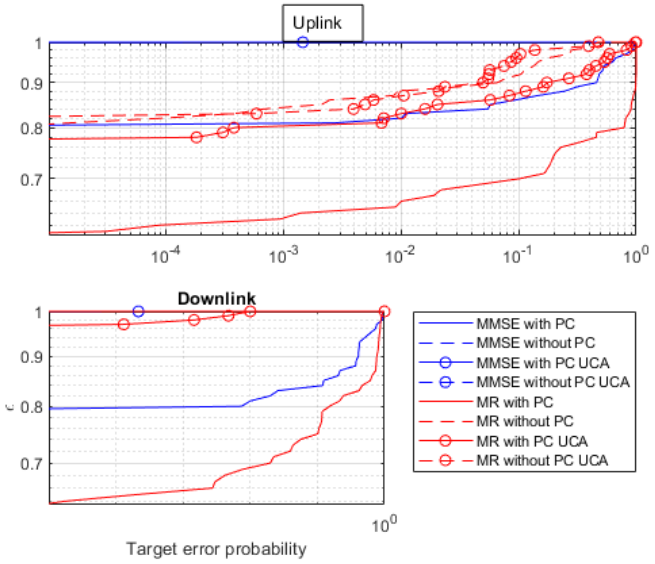

Fig. 5.3: Network availability η with and without pilot contamination.(a) Uplink transmission. (b) Downlink transmission.

it is observed that probability of error for UCA is better than probability of error when ULA is used. But, the advantage of UCA comes at a cost, sometimes the processing techniques that are used for ULA may not directly extend to UCA.

5.3 Network Availability for the case of 4 Cell 10 UEs each Massive MIMO

L = 4 square cells, each of size 75m$\times$75m, make up the simulation setup containing K = 10 UEs each, within the cell, independently and uniformly dispersed, a distance of at least 5 metres from the BS. A horizontal ULA is evaluated with M = 100 antennas with half wavelength separation, similar to the Two UE Single Cell Massive MIMO scenario analysis. Each UE's correlation matrix and large scale fading coefficient follow the models in (39) and (40), respectively. As in [mas, Sec. 4.1.3], a wrap-around topology is used. Parameters are n = 300, b = 160 and transmit power both in uplink and downlink is 10 dBm.

In fig A.1, network availability (41) for a fixed $\epsilon_{target} = 10^{-5}$ versus the number

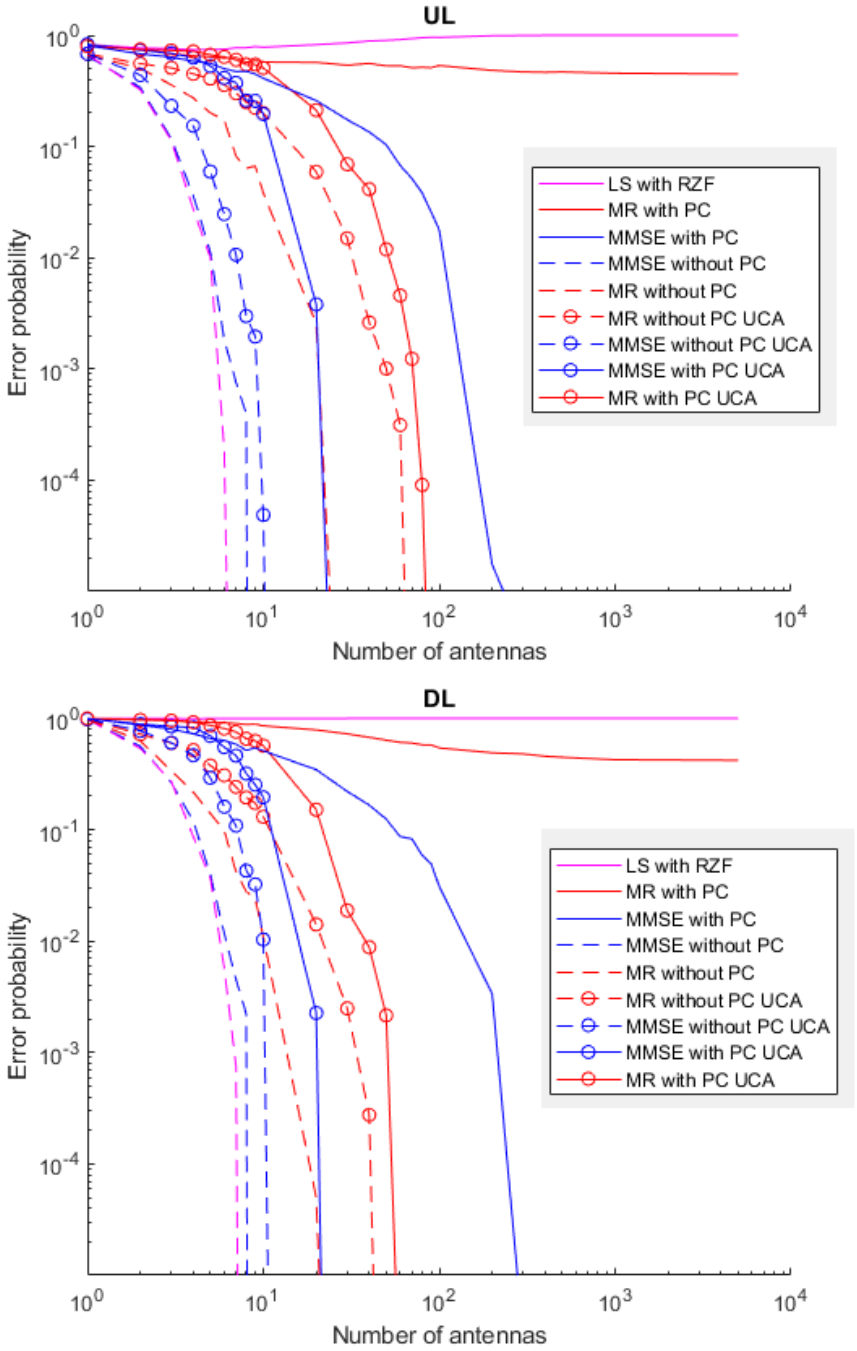

Fig. 5.4: Average error probability of UE1 versus number of antennas M with and without pilot contamination. (a) Uplink transmission. (b) Downlink transmission.

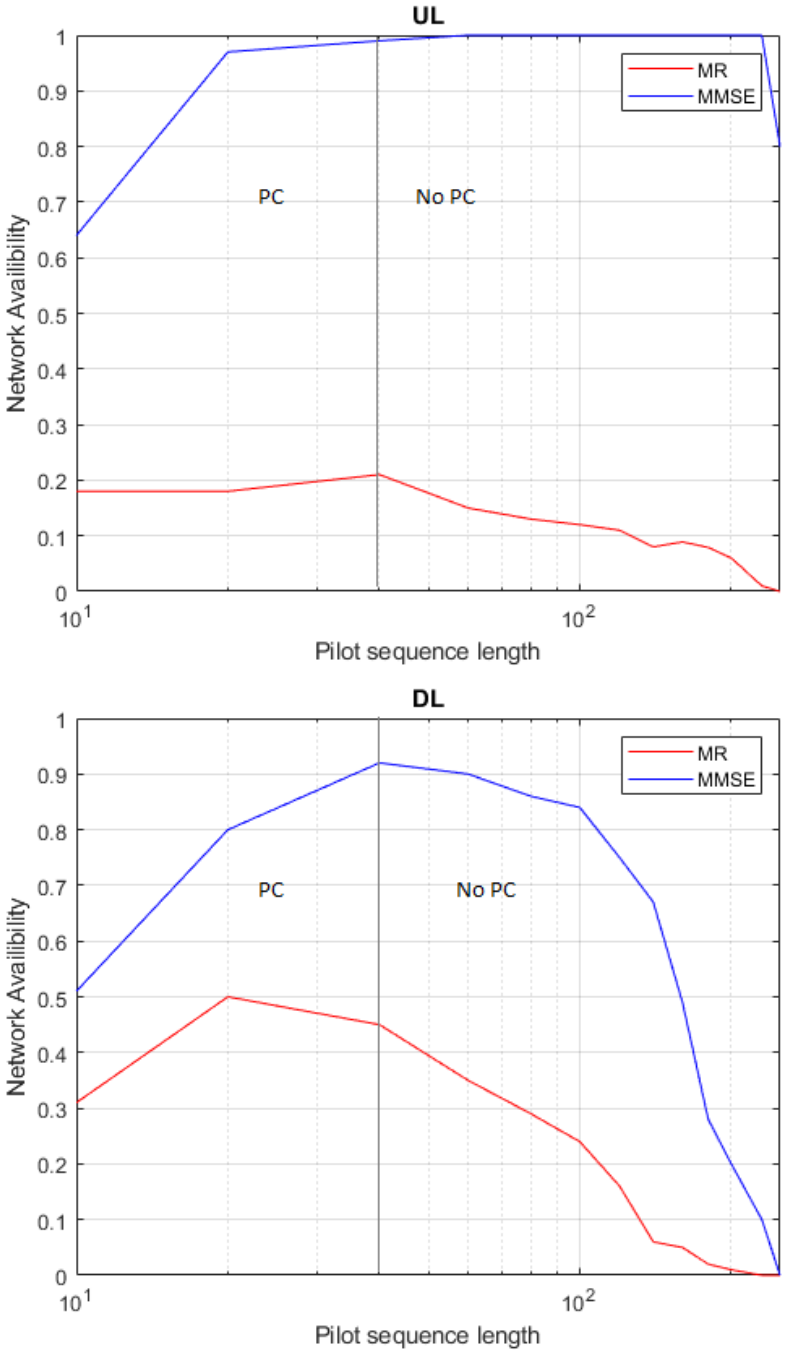

Fig. 5.5: Network availability for $\epsilon_{target} = 10^{-5}$. (a) Uplink transmission. (b) Downlink transmission.

of pilot symbols $n_p = fK$, is plotted where f is the pilot reuse factor is implemented in line with fbl. Fig A.1 verifies that pilot contamination should be avoided and that MMSE should be used instead of MR in most cases. With multicell MMSE in Uplink and Downlink, a network availability of above 90 percent can be attained by setting a pilot reuse factor of f = 4 such that $n_p = fK = 40$. In a network with L = 4 cells, this number of n_p is the smallest that prevents pilot contamination. However, increasing n_p has a negative impact on network availability, particularly in the downlink. Indeed, the benefits of a more accurate CSI are negated by the corresponding reduction in the number of channel uses $n_{dl} = (300n_p)/2$ available for data transmission in the DL. With multicell MMSE processing, the performance difference between UL and DL is due to the assumption that the UE has no CSI and performs mismatched decoding by relying on channel hardening. Additional network availability benefits can be achieved by increasing the number of BS antennas, scheduling to avoid serving UEs that are difficult to separate spatially using linear precoding at the same time, or reducing the number of UEs served simultaneously. Even when there is no pilot contamination, network availability achieved with MR is less than 50 percent, implying that MR precoding/combining is too susceptible to interference to satisfy the low error probability targets necessary in low latency networks like URLLC. If no channel covariance matrix is available at the receiver, then LS estimator and RLF combining is used.

CHAPTER 6

CONCLUSION

Specifically, for a BS with upto 100 antennas, it is crucial to avoid pilot contamination and to employ MMSE precoding/combining instead of computationally less intensive MR precoding/combining . If the receiver does not have such access, the BS can do least square channel estimation followed by regularised zero forcing with a performance penalty. This is based on a finite-blocklength information theory-based firm nonasymptotic bound on the error probability and its application to a realistic Massive MIMO network with imperfect channel state information (I-CSI), spatially correlated channels, arbitrary linear spatial processing, pilot contamination, and randomly positioned UEs. An accurate approximation for error probability bound based on the saddlepoint method which is computationally efficient for the low error probabilities targeted in URLLC applications is implemented in line with fbl. In addition to that, Error probability and network availability in the case of single cell two UE Massive MIMO case with and without pilot contamination with UCA is also simulated. But, the advantage of UCA comes at a cost, sometimes the processing techniques that are used for ULA may not directly extend to UCA.

APPENDIX A

Golden section search

The RCU bound of error probability is assessed using the saddlepoint approximation in all numerical simulations presented and optimised it over the parameter s using a golden section search. Below is snippet of code

```
while ((abs(END_INT-START_INT)>TOL) && (k<iter))

    if f_x1 < f_x2 %function smaller in x1 than in x2
        END_INT = x2; %make interval smaller
        x2 = x1; %set new end of interval
        x1 = START_INT+(1-tau)*(END_INT-START_INT); %find new beginning

        f_x2 = f_x1;%already have value in x1
        f_x1 = f(x1);%compute new value for new beginning

    else
        START_INT=x1; %function smaller in x2 than in x1 so set new start indx to x1
        x1 = x2; %replace as new start index
        x2=START_INT+tau*(END_INT-START_INT); %compute new end index

        f_x1= f_x2;
        f_x2 = f(x2);
    end


    k=k+1;
end
```

Fig. A.1: Golden section search code snippet

REFERENCES

1. (). Fundamentals of massive mimo. https://www.cambridge.org/core/books/fundamentals-of-massive-mimo/C43AF993A6DA7075EC5F186F6BAC914B.

2. (). Information theory and reliable communication. newyork, ny, u.s.a.: John wiley and sons, 1968,. http://gr.xjtu.edu.cn/c/document_library/get_file?folderId=2422385&name=DLFE-98012.pdf.

3. (). An introduction to probability theory and its applications,2nd ed.,. http://www.ru.ac.bd/stat/wp-content/uploads/sites/25/2019/03/101_06_Feller_An-Introduction-to-Probability-Theory-and-Its-Applications-Vol.-2.pdf.

4. (). Massive mimo networks: Spectral, energy, and hardware efficiency. https://raw.githubusercontent.com/emilbjornson/massivemimobook/master/massive_MIMO_networks.pdf.

5. (). Service requirements for cyber-physical control applications in vertical domains. https://www.etsi.org/deliver/etsi_ts/122100_122199/122104/16.05.00_60/ts_122104v160500p.pdf.

6. (). unified approach to gaussian channels with finiteblocklength. https://curate.nd.edu/show/df65v694z4h.

7. (). Urllc with massive mimo:analysis and design at finite blocklength. https://arxiv.org/pdf/2009.10550.pdf.

8. **Bana, A.-S.**, **G. Xu**, **E. D. Carvalho**, and **P. Popovski** (2018). Ultra reliable low latency communications in massive multi-antenna systems. *In 2018 52nd Asilomar Conference on Signals, Systems, and Computers*. doi:10.1109/ACSSC.2018.8645402.

9. **Biglieri, E.**, **J. Proakis**, and **S. Shamai** (1998). Fading channels: information-theoretic and communications aspects. *IEEE Transactions on Information Theory*, **44**(6), 2619–2692, doi:10.1109/18.720551.

10. **Björnson, E.**, **J. Hoydis**, and **L. Sanguinetti** (2018). Massive mimo has unlimited capacity. *IEEE Transactions on Wireless Communications*, **17**(1), 574–590, doi:10.1109/TWC.2017.2768423.

11. **Björnson, E.**, **L. Sanguinetti**, and **M. Debbah** (2016). Massive mimo with imperfect channel covariance information. *In 2016 50th Asilomar Conference on Signals, Systems and Computers*. doi:10.1109/ACSSC.2016.7869195.

12. **Durisi, G.**, **T. Koch**, and **P. Popovski** (2016*a*). Toward massive, ultrareliable, and low-latency wireless communication with short packets. *Proceedings of the IEEE*, **104**(9), 1711–1726, doi:10.1109/JPROC.2016.2537298.

13. **Durisi, G.**, **T. Koch**, **J. Östman**, **Y. Polyanskiy**, and **W. Yang** (2016*b*). Short-packet communications over multiple-antenna rayleigh-fading channels. *IEEE Transactions on Communications*, **64**(2), 618–629, doi:10.1109/TCOMM.2015.2511087.

14. **Haenggi, M.** (2016). The meta distribution of the sir in poisson bipolar and cellular networks. *IEEE Transactions on Wireless Communications*, **15**(4), 2577–2589, doi:10.1109/TWC.2015.2504983.

15. **Hoydis, J.**, **S. ten Brink**, and **M. Debbah** (2011). Massive mimo: How many antennas do we need? *In 2011 49th Annual Allerton Conference on Communication, Control, and Computing (Allerton)*. doi:10.1109/Allerton.2011.6120214.

16. **Kaplan, G.**, **S. Shamai**, and **ha-Tekhniyon Makhon tekhnologi le-Yisra'el. ha-Fakultah le-handasat hashmal** (1991). *Information Rates and Error Exponents of Compound Channels with Application to Antipodal Signaling in a Fading Environment*. EE publication [series]. Technion-I.I.T., Department of Electrical Engineering. URL https://books.google.co.in/books?id=Xq8hnwEACAAJ.

17. **Karlsson, M.**, **E. Björnson**, and **E. G. Larsson** (2018). Performance of in-band transmission of system information in massive mimo systems. *IEEE Transactions on Wireless Communications*, **17**(3), 1700–1712, doi:10.1109/TWC.2017.2784809.

18. **Lancho, A.**, **T. Koch**, and **G. Durisi** (2020*a*). On single-antenna rayleigh block-fading channels at finite blocklength. *IEEE Transactions on Information Theory*, **66**(1), 496–519, doi:10.1109/TIT.2019.2945782.

19. **Lancho, A.**, **J. Östman**, **G. Durisi**, **T. Koch**, and **G. Vazquez-Vilar** (2020*b*). Saddlepoint approximations for short-packet wireless communications. *IEEE Transactions on Wireless Communications*, **19**(7), 4831–4846, doi:10.1109/TWC.2020.2987573.

20. **Lapidoth, A.** and **S. Shamai** (1999). Fading channels: how perfect need "perfect side information" be? *In Proceedings of the 1999 IEEE Information Theory and Communications Workshop (Cat. No. 99EX253)*. doi:10.1109/ITCOM.1999.781400.

21. **Larsson, E. G.**, **O. Edfors**, **F. Tufvesson**, and **T. L. Marzetta** (2014). Massive mimo for next generation wireless systems. *IEEE Communications Magazine*, **52**(2), 186–195, doi:10.1109/MCOM.2014.6736761.

22. **Martinez, A.** and **A. G. i Fàbregas** (2011). Saddlepoint approximation of random-coding bounds. *In 2011 Information Theory and Applications Workshop*. doi:10.1109/ITA.2011.5743590.

23. **Marzetta, T. L.** (2010). Noncooperative cellular wireless with unlimited numbers of base station antennas. *IEEE Transactions on Wireless Communications*, **9**(11), 3590–3600, doi:10.1109/TWC.2010.092810.091092.

24. **Polyanskiy, Y.**, **H. V. Poor**, and **S. Verdu** (2010). Channel coding rate in the finite blocklength regime. *IEEE Transactions on Information Theory*, **56**(5), 2307–2359, doi:10.1109/TIT.2010.2043769.

25. **Popovski, P.**, **K. F. Trillingsgaard**, **O. Simeone**, and **G. Durisi** (2018). 5g wireless network slicing for embb, urllc, and mmtc: A communication-theoretic view. *IEEE Access*, **6**, 55765–55779, doi:10.1109/ACCESS.2018.2872781.

26. **Ren, H.**, **C. Pan**, **Y. Deng**, **M. Elkashlan**, and **A. Nallanathan** (2020). Joint pilot and payload power allocation for massive-mimo-enabled urllc iiot networks. *IEEE Journal on Selected Areas in Communications*, **38**(5), 816–830, doi:10.1109/JSAC.2020.2980910.

27. **Sanguinetti, L.**, **E. Björnson**, and **J. Hoydis** (2020). Toward massive mimo 2.0: Understanding spatial correlation, interference suppression, and pilot contamination. *IEEE Transactions on Communications*, **68**(1), 232–257, doi:10.1109/TCOMM.2019.2945792.

28. **Scarlett, J.**, **A. Martinez**, and **A. G. i. Fabregas** (2014). Mismatched decoding: Error exponents, second-order rates and saddlepoint approximations. *IEEE Transactions on Information Theory*, **60**(5), 2647–2666, doi:10.1109/TIT.2014.2310453.

29. **Yang, W.**, **G. Durisi**, **T. Koch**, and **Y. Polyanskiy** (2014). Quasi-static multiple-antenna fading channels at finite blocklength. *IEEE Transactions on Information Theory*, **60**(7), 4232–4265, doi:10.1109/TIT.2014.2318726.

30. **Zeng, J.**, **T. Lv**, **R. P. Liu**, **X. Su**, **Y. J. Guo**, and **N. C. Beaulieu** (2020). Enabling ultrareliable and low-latency communications under shadow fading by massive mu-mimo. *IEEE Internet of Things Journal*, **7**(1), 234–246, doi:10.1109/JIOT.2019.2945106.

31. **Östman, J.**, **G. Durisi**, **E. G. Ström**, **M. C. Coşkun**, and **G. Liva** (2019). Short packets over block-memoryless fading channels: Pilot-assisted or noncoherent transmission? *IEEE Transactions on Communications*, **67**(2), 1521–1536, doi:10.1109/TCOMM.2018.2874993.